Asynchronous Inelastic Scattering of Electrons at the Ponderomotive Potential of Optical Waves

Martin Kozák* and Tomáš Ostatnický
Faculty of Mathematics and Physics, Charles University, Ke Karlovu 3, 12116 Prague 2, Czech Republic

(Received 28 January 2022; accepted 13 June 2022; published 6 July 2022)

We study free electron dynamics during inelastic interaction with the ponderomotive potential of a traveling optical wave using classical and quantum-mechanical models. We show that in the strong interaction regime, the electrons trapped in the periodic potential oscillate leading to periodic revolutions of sharp peaks of the density distributions in the real and momentum spaces. In this regime, the synchronicity between the velocity of the optical wave and the electron propagation velocity is not required. Asynchronous interaction enables acceleration or deceleration of a significant fraction of the electrons to a final spectrum with a relative spectral width of 0.5%–2.5%. This technique allows one to accelerate electrons from rest to keV energies while reaching a narrow spectrum of kinetic energies and femtosecond pulsed operation.

DOI: 10.1103/PhysRevLett.129.024801

Inelastic interaction between freely propagating electrons and light has become a widely studied topic in the last two decades because it enables quantum coherent control of the electron wave function in electron microscopes [1–6], attosecond compression of electron pulses for time-resolved experiments [7–11], control of transverse distribution of electrons [12–19], or electron acceleration [20,21]. Pulsed electron beams and modulated electron wave packets have many interesting applications such as ultrafast electron diffraction [22,23], photon-induced near-field electron microscopy [24,25], attosecond time-resolved imaging of optical and plasmonic fields [5,6], coherent excitation of two-level systems [26,27], studies of coherent cathodoluminescence [28,29], or quantum information processing [30,31]. Various control mechanisms allowing to tune the electron-photon interaction have been recently studied including different coupling schemes [16,32–35], shaped light fields [4,36], or modified photon statistics of the driving light [37].

An essential assumption in all the schemes aiming for photon-mediated electron scattering has been the initial synchronicity between the propagation velocities of the electron and an effective potential acting on the electrons, which is a harmonic function of the coordinate along the electron propagation. Moreover, the theoretical description has typically assumed the approximation of negligible change of the electron's velocity during the interaction (nonrecoil approximation). The strong interaction regime has been studied only recently for the case of electrons interacting with optical near fields [38,39].

In this Letter we study the regime of electron interaction with the effective ponderomotive potential generated by the far-field optical radiation beyond the limit of a weak perturbation and we predict several unexpected observations. We show that a part of the electron distribution located initially close to the minimum of the potential undergoes harmonic oscillations. This leads to periodic focusing and defocusing of the electron distributions in both the real and momentum spaces. When the initial velocities of the electrons and the potential are not equal, a sharp peak in the electron energy spectrum displaced from the initial electron energy can be generated. By making the traveling optical wave faster than the electrons, it is possible to accelerate a significant portion of the electrons and reach a narrow final spectrum, which is not possible in the synchronous case.

An electron propagating in vacuum interacts with electromagnetic fields via Lorentz force. However, in the case of a single optical plane wave, photon absorption would not lead to a net momentum change of the electron due to a mismatch between the phase velocity of the light wave propagating at the speed of light c and the group velocity of the electron $v_0 < c$. To efficiently gain photon energy by electrons, the amplitude or phase of the electromagnetic field has to be spatially modulated by scattering at nanostructures with feature sizes smaller than the wavelength of the driving wave [1,25] or by the interference of two or more light waves [7,40]. In the first case, the generated optical near field contains a broad spectrum of evanescent waves propagating along the nanostructure at subluminal velocities that can be phase matched to the electrons. The latter type of interaction is mediated by the ponderomotive potential $U_p = e^2|\boldsymbol{\xi}|^2/(4m_0\omega^2)$ (nonrelativistic expression), which corresponds to the time-averaged kinetic energy of the electron during its quiver motion in an oscillating electromagnetic field (see Ref. [41] for details). Here $\boldsymbol{\xi}$ and ω are the complex electric field amplitude and frequency of the light wave and e and m_0 are the electron charge and rest mass, respectively. When

 © 2022 American Physical Society

the ponderomotive potential is spatially modulated, the associated force pushes the electrons out of the regions of high light intensity. This effect has been considered for the elastic coherent electron scattering at an optical standing wave [12–14], inelastic scattering of electrons at high-intensity optical fields [42,43], and for inelastic scattering at a traveling wave formed by two light fields oscillating at different frequencies [7,44,45].

The scheme proposed in this Letter assumes that the electrons interact with the ponderomotive potential of an optical traveling wave generated by two counterpropagating mutually coherent light waves at different frequencies, which in the case of synchronous interaction fulfill the relation $v_w = v_0 = c(\omega_1 - \omega_2)/(\omega_1 + \omega_2)$, where v_w is the velocity of the traveling wave, v_0 is the initial electron velocity, c is speed of light, and ω_1 and ω_2 are the angular frequencies of the two light waves. A high degree of coherence together with strong electromagnetic field then requires understanding of the dynamics in terms of strong resonant interaction beyond the perturbation description, like Rabi oscillations in two-level systems. This explains the efficiency of the momentum conversion in the system. Examples of possible implementation are a combination of two waves at harmonic frequencies of a common fundamental wavelength or signal and idler pulses from an optical parametric amplifier pumped by femtosecond laser pulses from an ytterbium-doped solid-state laser with fundamental wavelength of 1030 nm. These lasers allow us to reach both sufficient pulse energy of several hundreds of μJ (field amplitudes of the order of 10^{10} V/m generate potential with amplitude ~100 meV) and the high repetition rate necessary to perform the experiments with pulsed electron beams.

The proposed geometry is shown in Fig. 1(a) and can be generalized for different angles of incidence of the light waves [7,41]. The energy and momentum conservation laws during a single stimulated scattering event are fulfilled by simultaneous absorption of a photon from one wave generating the ponderomotive potential and stimulated emission of a photon to the other wave [7], which can be visualized in the dispersion diagram of the free electron and free photon [Fig. 1(b)]. In such stimulated Compton scattering, the electron energy shifts by integer multiples of $\Delta E = \hbar(\omega_1 - \omega_2)$. The momentum shift in the case of counterpropagating waves is $\Delta\mathbf{p} = \hbar(\mathbf{k}_1 - \mathbf{k}_2)$, where $\mathbf{k}_1 = \hat{\mathbf{z}}\omega_1/c$ and $\mathbf{k}_2 = -\hat{\mathbf{z}}\omega_2/c$ are the wave vectors of the two waves and $\hat{\mathbf{z}}$ is the unit vector along z coordinate. For electrons traveling in the direction of $\hat{\mathbf{z}}$, the transverse momentum change is zero. The optical traveling wave has an effective linear dispersion [dashed red line in the insets of Fig. 1(b)], which is similar to the dispersion of retarded photons [25].

In the asynchronous interaction regime characterized by $v_w \neq v_0$, the effective dispersion of the wave is not tangential to the electron dispersion curve [blue dashed line in the lower inset of Fig. 1(b)]. The energy and momentum conservation laws are thus not fulfilled for a scattering event in which only two photons interact with the electron but can be fulfilled when many photons are absorbed and emitted in the same time. Assuming that $v_w > v_0$, the electron can jump to a state with higher energy (when $v_w < v_0$ to a lower-energy state), in which the wave dispersion intersects with the electron dispersion. Because there is only one intersection displaced from the initial electron energy, the electron energy shift is unidirectional, e.g., either acceleration or deceleration depending on the sign of the difference $v_0 - v_w$. For more detailed discussion of conservation laws, see Section II of [41].

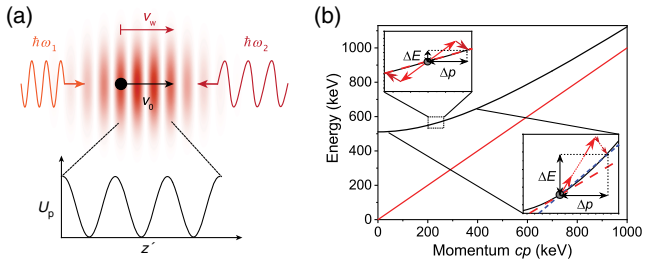

FIG. 1. (a) Layout of the proposed experiment. Two counterpropagating light waves with photon energies $\hbar\omega_1$ and $\hbar\omega_2$ generate a harmonic ponderomotive potential propagating at velocity v_w, which interacts with the electron with velocity v_0. (b) Dispersion relations of a free electron (black curve) and a free photon (red line). Upper inset: energy and momentum conservation for synchronous interaction ($v_0 = v_w$). Lower inset: strong interaction regime for the synchronous case (red dashed line) and asynchronous case (blue dashed line). While the wave dispersion is tangential to the electron dispersion in the synchronous case, in the asynchronous case there appears a crossing point with the electron dispersion displaced from the initial electron energy.

To understand the underlying physics, we describe the electron dynamics using a simplified 1D classical and semiclassical models with the effective ponderomotive potential of a traveling wave. We note that in the selected geometry, the ponderomotive potential does not depend on the transverse coordinates (directions perpendicular to the electron trajectory) and the 1D model is fully justified. It can also be applied in a more general case of nonzero angles of incidence of the two light waves (see Fig. S2 in [41]) providing that the conditions for zero transverse momentum change of the electrons are fulfilled [7]. We assume homogeneous initial distribution of the electrons in space (electrons are randomly distributed along the propagation direction) and the distribution in momentum space characterized by Gaussian function with center kinetic energy $E_0 = 1/2m_0v_0^2$ and full width at half maximum width of δE_0. The potential of the optical traveling wave has a form of $U_p(z,t) = A/2\{1 - \cos[2\pi(v_w t - z)/\Lambda]\}$, where A is the amplitude of the potential, Λ is its spatial period, and v_w is the velocity of the wave in the laboratory frame.

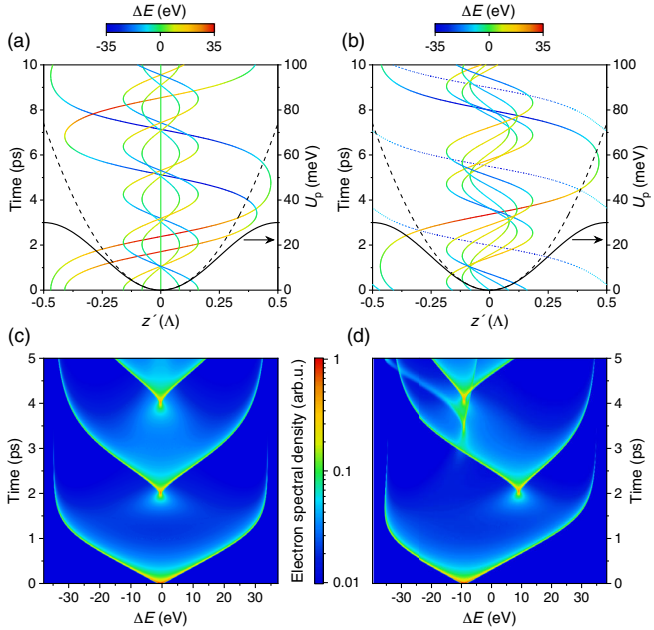

FIG. 2. The trajectories (curves) of electrons in the ponderomotive potential of an optical traveling wave with period $\Lambda = 206$ nm for (a) $\Delta E_0 = 0$ and (b) $\Delta E_0 = -9$ eV, $v_w = 0.2c$, and $A = 30$ meV. The color scale shows the instantaneous energy shift $\Delta E = E(t) - E_0$. Dotted curves in (b) show the trajectory of an electron, which is not captured within one period of the potential. The full potential (solid curve) and parabolic approximation (dashed) are shown for comparison. Electron spectra as a function of time for the synchronous (c) and asynchronous (d) cases assuming initial energy distribution with the width of 0.5 eV.

We investigate the electron dynamics in the frame connected to the traveling wave, in which the potential is stationary, by using Galilean transformation for the electron coordinate $z' = z - v_w t$ and velocity $v' = v - v_w$, and assuming that U_p with constant amplitude A is switched on at time $t = 0$ (generalization to time-dependent amplitude is obtained using numerical simulations, see Ref. [41], Section V).

In the analytical theory we restrict ourselves to subrelativistic phenomena with low-energy electrons (Lorentz factor $\gamma \sim 1$). The classical trajectories of individual electrons in the potential $U_p(z')$ are calculated by integrating the classical equation of motion $m_0 \ddot{z}' + \nabla U_p(z') = 0$ with the initial condition $v_0' = v_0 - v_w$. This equation is nothing but the equation describing a nonlinear pendulum, for which the analytical solution was discussed elsewhere [46]. We solve kinetic equations by numerical integration using fourth-order Runge-Kutta algorithm.

We compare the electron trajectories for the synchronous case $v_0' = 0$ [Fig. 2(a)] and asynchronous case $v_0' < 0$ [Fig. 2(b)]. The potential is approximately parabolic for a significant part of the electrons located close to its minimum. The dynamics of these electrons can be described analytically by solving the equation of motion with the potential $U_p^{\mathrm{par}}(z') = \pi^2 A z'^2/\Lambda^2$. The solution of a classical linear harmonic oscillator leads to periodic oscillations of the electrons in both the real and momentum spaces. The trajectories of these electrons are focused at times $t_{z'} = (2k+1)T/4$, where $T = 2\pi/\Omega$ is the temporal period of the oscillations, $k = 0, 1, 2, \ldots$ and $\Omega = \sqrt{2\pi^2 A/(\Lambda^2 m_0)}$ is the oscillation frequency. In contrast, the trajectories in the momentum space are focused in times $t_{v'} = kT/2$, in which all the electrons from the parabolic region of the potential have the same energy, which is illustrated by the color scale in Figs. 2(a) and 2(b).

In the synchronous case shown in Fig. 2(a), the foci of the spatial trajectories are located in the coordinate corresponding to the minimum of the potential. The time evolution of the electron velocity in the rest frame of the wave can be expressed as $v' = v_0' \cos(\Omega t) - z_0' \Omega \sin(\Omega t)$, where z_0' is the initial electron position. For $v_0' = 0$, the velocity of all the electrons in times $t_{v'}$ is $v' = v_0' = 0$. An interesting result is obtained for the asynchronous case $v_0' < 0$, in which the velocity of all the electrons in times $t_{v'}$ is oscillating between two values, v_0' and $-v_0'$. The latter corresponds to electrons accelerated by $2|v_0'|$. When the potential generated by the optical waves is switched off in time $t = (2k+1)T/2$, the electrons from the central part of the potential are all accelerated to the same final kinetic energy.

This is shown in Figs. 2(c) and 2(d), where we plot the temporal evolution of the electron spectra assuming the full ponderomotive potential U_p with the amplitude $A = 30$ meV, which is generated by the second and third harmonics of the fundamental output of the Yb:KGW laser with the wavelengths of 343 nm and 515 nm leading to $\Lambda = 206$ nm and $v_w = 0.2c$. In the synchronous case shown in Fig. 2(c), the kinetic energy corresponding to an electron synchronous with the wave E_w is equal to the initial kinetic energy of the electrons $E_0 = 10.537$ keV ($v_0 = 0.2c$). The energy difference is defined as $\Delta E(t) = E(t) - E_w$, where $E(t)$ is the instantaneous kinetic energy of the electron. In Fig. 2(d) we show the asynchronous case, in which $\Delta E(t = 0) = \Delta E_0 = -9$ eV. In both cases, the electron spectrum reaches its narrowest distribution approximately in time $t_{v'}$ which is a function of both the potential amplitude A and the period Λ. In the asynchronous case, the main spectral peak is clearly shifted from the initial electron energy.

Electron spectra for fixed $A = 30$ meV and different initial excess energies ΔE_0 are plotted in Fig. 3(a) at a time corresponding to the narrowest spectrum of accelerated electrons. We observe that the electron acceleration is reliable and produces narrow energy distribution up to the situation when a majority of the electrons have enough energy to propagate freely within the periodic potential [an example of such trajectory is shown as dotted curve in Fig. 3(b)]. As a consequence, we can see a buildup of a new

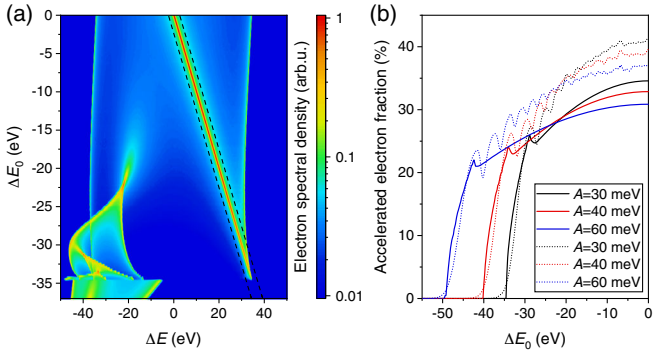

FIG. 3. (a) Electron energy spectra at time corresponding to the narrowest spectrum of accelerated electrons for different initial energy difference from synchronized state ΔE_0, $A = 30$ meV. (b) Accelerated electron fraction [electrons from the region marked by dashed lines in (a)] versus ΔE_0 for different heights of the ponderomotive potential. Curves plotted for classical (solid) and quantum (dotted) models.

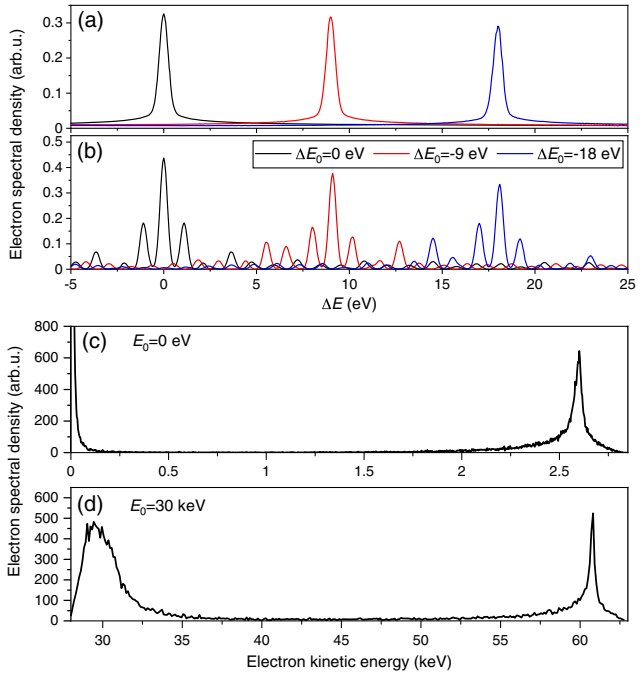

FIG. 4. Comparison of the electron spectra at time corresponding to the narrowest spectrum of accelerated electrons for different potentials and initial electron energies calculated by classical (a) and quantum models (b). Spectra of electrons accelerated by the ponderomotive potential of a traveling optical wave (c) from rest and (d) from the initial energy of 30 keV. Spectra are calculated using classical relativistic simulations described in the text.

peak and the main peak vanishing for energies −20 eV and less. To illustrate the energy conversion efficiency we plot the accelerated electron fraction (i.e., the fraction of electrons within 6 eV window around the main peak) versus initial electron energy by solid lines in Fig. 3(b) for different potential amplitudes. Higher potentials clearly allow larger changes in the electron energy but, on the other hand, provide less efficiency. The breakdown of acceleration with decreasing ΔE_0 is due to the fact that the slow electrons are not captured within one period of the potential and their energy oscillates around the initial value.

To verify the role of quantum effects during the extended interaction of electrons with optical waves, we develop a semiclassical model based on the solution of the Schrödinger equation with the stationary potential in the rest frame of the wave (light fields are described classically). First we solve the stationary Schrödinger equation in the rest frame of the wave:

$$\left\{\frac{p^2}{2m} + \frac{A}{2}\left[1 - \cos\left(\frac{2\pi z'}{\Lambda}\right)\right]\right\}\psi_n(z') = E_n\psi_n(z'), \quad (1)$$

assuming $\psi_n(z') = \exp[ik_0'z'] \sum_{j=-\infty}^{+\infty} c_{nj} \exp[i2\pi jz'/\Lambda]$ due to the periodicity of the problem. We denote here k_0' the excess wave vector ($k_0' = mv_0'/\hbar$) and c_{nj} are expansion coefficients. We assign the energy E_n to the nth wave function $\psi_n(z')$ and finally the solution of the time-dependent Schrödinger equation can be written as

$$\Phi(z', t) = \sum_{n=0}^{\infty}\sum_{j=-\infty}^{+\infty} c_{n0}^* c_{nj} \exp\left[-\frac{iE_n t}{\hbar} + ik_0'z' + i\frac{2\pi jz'}{\Lambda}\right]. \quad (2)$$

This solution, in particular the term c_{n0}^*, assumes that the initial condition at $t = 0$ is an electron plane wave with wave vector k_0'. Solution in momentum space is found simply by taking the Fourier components of the real-space solution. The initial energy width of the electron distribution $\delta E_0 = 0.5$ eV is taken into account by evaluating the result of Eq. (2) for different initial electron energies with the weight given by the Gaussian distribution function.

The resulting electron spectra from the classical and semiclassical simulations are compared in Figs. 4(a) and 4(b). We plot the energy spectra at the time corresponding to the narrowest energy distribution of accelerated electrons for different initial electron energies and potential height of $A = 30$ meV. In the semiclassical model, the quantized nature of the interaction manifests itself via the peaks shifted from the initial electron energy by $\Delta E = \hbar(\omega_1 - \omega_2)$. These peaks are only present when $\delta E < \Delta E$ corresponding to the situation, in which the electron coherence length $l_{\mathrm{coh}} \sim v_0\hbar/\delta E$ is longer than the spatial period of the ponderomotive potential Λ.

To verify the practical applicability of the proposed extended interaction scheme, we perform full 3D simulations by solving the relativistic equation of motion of electrons with the Lorentz force $d/dt(\gamma m_0\mathbf{v}) = q(\boldsymbol{\xi} + \mathbf{v} \times \mathbf{B})$. Here $\gamma = 1/\sqrt{(1-\beta^2)}$ is the Lorentz factor, $\beta = |\mathbf{v}|/c$ and $\boldsymbol{\xi}$ and $\mathbf{B}$ are electric and magnetic fields of two femtosecond light pulses with Gaussian envelopes in space and time domains (details can be found in [41], Section III).

The resulting electron spectra for two specific cases are plotted in Figs. 4(c) and 4(d). The first simulation shows acceleration of the electrons from rest to the kinetic energy of $E = 2.57$ keV by using the traveling wave with $v_w = 0.05c$. The width of the spectral peak corresponding to the accelerated electrons is only $\delta E = 64$ eV (the relative spectral width is ~2.5%). Such quasimonochromatic electron pulses with duration of ~100 fs may find application in ultrafast time-resolved imaging experiments, in which the studied sample would be placed close to the source of the electrons to eliminate the dispersive temporal broadening of the electron pulse. In the second case we model the acceleration of electrons with initial kinetic energy of $E_0 = 30$ keV corresponding to $v_0 = 0.33c$. The velocity of the traveling wave is adjusted to $v_w = 0.388c$ and the electrons are accelerated to $E = 60.8$ keV with relative energy width of the peak of only ~0.5% (the parameters used in both simulations are described in [41], Section III and [47]). Combined with spectrally sensitive detection, such a scheme enables a new way of temporal gating of electrons for femtosecond time-resolved experiments by spectrally shifting them from the initial energy.

In conclusion, we describe a new regime of asynchronous interaction between freely propagating electrons and light mediated by the ponderomotive potential of an optical traveling wave. The possibility to generate narrow energy distributions of electrons spectrally shifted from the initial electron energy opens new opportunities in classical and quantum mechanical shaping of electron beams. The theory used here can be generalized to a case of injecting the electrons to an optical standing wave in a direction almost perpendicular to its wave vector. The role of the synchronicity is in such case transferred to the angle of incidence of the electrons with respect to the wave and the electrons can be accelerated unidirectionally in the transverse direction leading to a deflection under a certain angle. This regime is completely different from the coherent diffraction of electron waves at a periodic optical standing wave (Kapitza-Dirac effect) because it happens also in the classical regime within a point particle approximation. Besides the interaction with electrons, the ponderomotive force allows us to control neutral atoms or molecules [48], where the interaction can be enhanced by the presence of electronic resonances [49]. Our extended interaction scheme thus may offer a source of short pulses of neutral particles.

The authors would like to acknowledge the support by Czech Science Foundation (Project GA18-10486Y) and Charles University (Center of nano- and bio-photonics, UNCE/SCI/010, and PRIMUS/19/SCI/05).

*kozak@karlov.mff.cuni.cz

[1] F. J. García de Abajo, Rev. Mod. Phys. **82**, 209 (2010).
[2] A. Feist, K. E. Echternkamp, J. Schauss, S. V. Yalunin, S. Schäfer, and C. Ropers, Nature (London) **521**, 200 (2015).
[3] K. E. Priebe, C. Rathje, S. V. Yalunin, T. Hohage, A. Feist, S. Schäfer, and C. Ropers, Nat. Photonics **11**, 793 (2017).
[4] O. Reinhardt and I. Kaminer, ACS Photonics **7**, 2859 (2020).
[5] O. Kfir, H. Lourenço-Martins, G. Storeck, M. Sivis, T. R. Harvey, T. J. Kippenberg, A. Feist, and C. Ropers, Nature (London) **582**, 46 (2020).
[6] K. Wang, R. Dahan, M. Shentcis, Y. Kauffmann, A. Ben Hayun, O. Reinhardt, S. Tsesses, and I. Kaminer, Nature (London) **582**, 50 (2020).
[7] M. Kozák, T. Eckstein, N. Schönenberger, and P. Hommelhoff, Nat. Phys. **14**, 121 (2018).
[8] M. Kozák, N. Schönenberger, and P. Hommelhoff, Phys. Rev. Lett. **120**, 103203 (2018).
[9] G. M. Vanacore, I. Madan, G. Berruto, K. Wang, E. Pomarico, R. J. Lamb, D. McGrouther, I. Kaminer, B. Barwick, F. J. García de Abajo, and F. Carbone, Nat. Commun. **9**, 2694 (2018).
[10] P. Baum, J. Appl. Phys. **122**, 223105 (2017).
[11] Y. Morimoto and P. Baum, Nat. Phys. **14**, 252 (2018).
[12] P. L. Kapitza and P. A. Dirac, Math. Proc. Cambridge Philos. Soc. **29**, 297 (1933).
[13] D. L. Freimund, K. Aflatooni, and H. Batelaan, Nature (London) **413**, 142 (2001).
[14] H. Batelaan, Rev. Mod. Phys. **79**, 929 (2007).
[15] J. Handali, P. Shakya, and B. Barwick, Opt. Express **23**, 5236 (2015).
[16] M. Kozák, P. Beck, H. Deng, J. McNeur, N. Schönenberger, C. Gaida, F. Stutzki, M. Gebhardt, J. Limpert, A. Ruehl, I. Hartl, O. Solgaard, J. S. Harris, R. L. Byer, and P. Hommelhoff, Opt. Express **25**, 19195 (2017).
[17] M. Kozák, ACS Photonics **8**, 431 (2021).
[18] A. Feist, S. V. Yalunin, S. Schäfer, and C. Ropers, Phys. Rev. Research **2**, 043227 (2020).
[19] G. M. Vanacore, G. Berruto, I. Madan, E. Pomarico, P. Biagioni, R. J. Lamb, D. McGrouther, O. Reinhardt, I. Kaminer, B. Barwick, H. Larocque, V. Grillo, E. Karimi, F. J. García de Abajo, and F. Carbone, Nat. Mater. **18**, 573 (2019).
[20] J. Breuer and P. Hommelhoff, Phys. Rev. Lett. **111**, 134803 (2013).
[21] E. A. Peralta, K. Soong, R. J. England, E. R. Colby, Z. Wu, B. Montazeri, C. McGuinness, J. McNeur, K. J. Leedle, D. Walz, E. B. Sozer, B. Cowan, B. Schwartz, G. Travish, and R. L. Byer, Nature (London) **503**, 91 (2013).
[22] H. Ihee, V. A. Lobastov, U. M. Gomez, B. M. Goodson, R. Srinivasan, C. Y. Ruan, and A. H. Zewail, Science **291**, 458 (2001).
[23] B. J. Siwick, J. R. Dwyer, R. E. Jordan, and R. J. Miller, Science **302**, 1382 (2003).
[24] B. Barwick, D. J. Flannigan, and A. H. Zewail, Nature (London) **462**, 902 (2009).
[25] S. T. Park, M. Lin, and A. H. Zewail, New J. Phys. **12**, 123028 (2010).
[26] A. Gover and A. Yariv, Phys. Rev. Lett. **124**, 064801 (2020).
[27] B. Zhang, D. Ran, R. Ianconescu, A. Friedman, J. Scheuer, A. Yariv, and A. Gover, Phys. Rev. Lett. **126**, 244801 (2021).
[28] O. Kfir, V. D. Giulio, F. J. G. de Abajo, and C. Ropers, Sci. Adv. **7**, eabf6380 (2021).
[29] A. Karnieli, N. Rivera, A. Arie, and I. Kaminer, Sci. Adv. **7**, eabf8096 (2021).

[30] O. Reinhardt, C. Mechel, M. Lynch, and I. Kaminer, Ann. Phys. (Berlin) **533**, 2000254 (2021).
[31] A. Karnieli, N. Rivera, A. Arie, and I. Kaminer, Phys. Rev. Lett. **127**, 060403 (2021).
[32] N. V. Sapra, K. Y. Yang, D. Vercruysse, K. J. Leedle, D. S. Black, R. J. England, L. Su, R. Trivedi, Y. Miao, O. Solgaard, R. L. Byer, and J. Vučković, Science **367**, 79 (2020).
[33] R. Dahan, S. Nehemia, M. Shentcis, O. Reinhardt, Y. Adiv, X. Shi, O. Be'er, M. H. Lynch, Y. Kurman, K. Wang, and I. Kaminer, Nat. Phys. **16**, 1123 (2020).
[34] P. Yousefi, N. Schönenberger, J. Mcneur, M. Kozák, U. Niedermayer, and P. Hommelhoff, Opt. Lett. **44**, 1520 (2019).
[35] R. Shiloh, T. Chlouba, P. Yousefi, and P. Hommelhoff, Opt. Express **29**, 14403 (2021).
[36] A. Konečná and F. J. García de Abajo, Phys. Rev. Lett. **125**, 030801 (2020).
[37] R. Dahan, A. Gorlach, U. Haeusler, A. Karnieli, O. Eyal, P. Yousefi, M. Segev, A. Arie, G. Eisenstein, P. Hommelhoff, and I. Kaminer, Science **373**, eabj7128 (2021).
[38] N. Talebi, Phys. Rev. Lett. **125**, 080401 (2020).
[39] N. Talebi, Adv. Phys. X **3**, 1499438 (2018).
[40] M. Kozák, Phys. Rev. Lett. **123**, 203202 (2019).
[41] See Supplemental Material at http://link.aps.org/supplemental/10.1103/PhysRevLett.129.024801 for the details of the theory and numerical calculations with finite temporal width of optical fields and for the discussion of the momentum and energy conservation in the asynchronous interaction.
[42] P. H. Bucksbaum, M. Bashkansky, and T. J. McIlrath, Phys. Rev. Lett. **58**, 349 (1987).
[43] P. H. Bucksbaum, D. W. Schumacher, and M. Bashkansky, Phys. Rev. Lett. **61**, 1182 (1988).
[44] V. Haroutunian and H. Avetissian, Phys. Lett. A **51**, 320 (1975).
[45] P. Baum and A. H. Zewail, Proc. Natl. Acad. Sci. U.S.A. **104**, 18409 (2007).
[46] K. Ochs, Eur. J. Phys. **32**, 479 (2011).
[47] B. Quesnel and P. Mora, Phys. Rev. E **58**, 3719 (1998).
[48] U. Eichmann, T. Nubbemeyer, H. Rottke, and W. Sandner, Nature (London) **461**, 1261 (2009).
[49] P. L. Gould, G. A. Ruff, and D. E. Pritchard, Phys. Rev. Lett. **56**, 827 (1986).